REACTIONS BETWEEN Al_2O_3/MgO CRUCIBLE MATERIALS AND A VACUUM MELTED Hf-BEARING SUPERALLOY

W. H. Sutton
W. A. Johnson
Special Metals Co., New Hartford, N.Y.

Chemical reactions between a Hf-bearing superalloy melt and crucibles of three Al_2O_3/MgO base compositions were investigated. The Al, Zr, and Hf in the melt reacted with the oxygen generated by the breakdown of the crucible materials. The details of the reactions and the influence of crucible instability on the oxide content in the skull and in cast ingots are discussed.

INTRODUCTION

Melting superalloys under vacuum suppresses the normal oxidation of the alloying elements because of the low oxygen pressure in the furnace. However, the low furnace pressure, typically $<10 \times 10^{-3}$ torr, favors the decomposition of oxide crucible materials, which in turn, provides a steady flux of oxygen into the melt. Vaughn and Geiger showed that the aluminum in nickel-base alloys containing Al, Ti and C would react with this oxygen source to form Al_2O_3 particles in melts contained in either Al_2O_3 or MgO crucibles (1).

Hafnium, being a more powerful deoxidizer than Al, will directly reduce Al_2O_3 to form HfO_2 (2,3). Thus Hf-bearing alloys are more prone to form inclusions during melting. This paper presents the results of an investigation on the reactions which occurred between reactive alloying elements (Al, Ti, Hf, Zr) in melts of an advanced superalloy and crucibles of MgO, Al_2O_3, and $MgAl_2O_4$ (spinel) compositions.

EXPERIMENTAL PROCEDURE

The compositions of the materials used in this study are presented in Table I. A nickel melt was made in each of the crucibles to precondition them prior to melting the alloy.

One heat was melted without the reactive adds (Al, Ti, Zr, and Hf) to provide a base-line for comparison.

Table I. Composition of Materials Used in the Experiments

(1)	Composition							Porosity
Crucible	Al_2O_3	MgO	SiO_2	CaO	Fe_2O_3	TiO_2	Na_2O	%
Al_2O_3-P	99.55	--	0.07	--	0.09	--	0.25	21
MgO-R	6.5	92.0	1.3	--	--	--	--	20
Spinel-R	70.60	28.20	0.30	0.35	0.05	0.01	0.35	21

Alloy	Ni	Cr	Co	Mo	Cb	B	C	Al	Ti	Zr	Hf
	54.15	12.40	18.50	3.10	1.65	.02	.02	5.00	4.30	.06	.80

(1)P = Prefire, R = Ram

Approximately 136Kg (300 lb.) charges were made from the same lots of raw materials, and were all melted under the same conditions, 1500°C (2730°F), 5-8 x 10^{-3} torr. The total melt time was about 100 minutes, and the reactive elements, Al, Ti, Zr, were added to the molten base charge about 35 minutes prior to the addition of the Hf. After the Hf add, the melts were poured into steel molds. The crucibles were allowed to cool under vacuum overnight, so that any metal or reactive products (skull) attached to the crucible would not be further oxidized. Additional details regarding the melting procedure and the characterization of the crucibles after use are discussed elsewhere (4).

All skulls from the alloy heats containing the reactive elements were removed and were examined by optical and SEM methods. The inclusion content of samples taken from cast ingots was determined by Pratt and Whitney using an electron beam remelting process to concentrate the oxides. These particles were then quantitatively extracted and weighed. The details of the inclusion analysis procedure have been reported previously (5), and are also described in this symposium (6).

RESULTS

Table II summarizes some of the experimental data. The oxygen content of the heat melted in the MgO crucible was significantly greater than that of the heats melted in the other two crucibles. The tendency of the alloy to wet the refractory materials was greatest in the case of the Al_2O_3 crucible, which could explain the strong adherence of the skull to the crucible.

Table II. Experimental Results

	At-Pour Chemistry					Contact(1)	At-Pour	(4)
Crucible	O	N(ppm)	C	Hf	Zr(%)	Angle(θ)°	Dross(3)	Skull
Al_2O_3	4	11	.020	.81	.07	78	10%	A
MgO	11	9	.024	.78	.06	133(2)	10%	B
Spinel	3	9	.018	.82	.06	100	10%	B

(1) Sessile drop contact angle; θ<90° = wetting (Ref. 4).
(2) Based on crucible sample containing 97% MgO.
(3) Dross = % melt surface covered with floating oxides.
(4) A = thick in regions, strongly adherent to crucible.
B = thin and continuous, weakly bonded.

Figure 1 shows cross sections of the skull and crucibles, and the depth of the altered region within the crucibles after the melt had been completed.

Figures 2A and 2B show SEM micrographs of the metal side of the Al_2O_3-crucible skull. Metal dendrites are quite obvious and contain fine oxides dispersed across the surface. A dendrite tip comprises the entire field of view in Figure 2B, the larger oxides tend to be Al_2O_3, while smaller ones are HfO_2.

The metal side of the Al_2O_3-crucible skull is distinctly different from that of the MgO-crucible skull shown in Figure 2C.

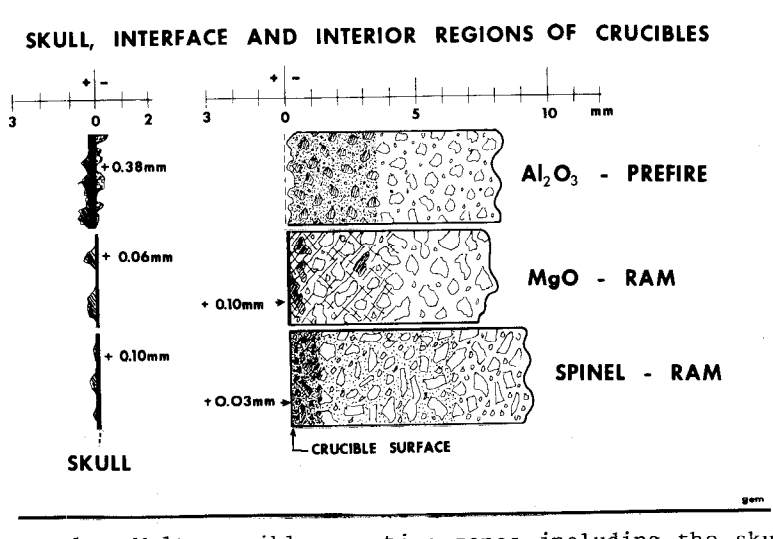

Figure 1. Melt-crucible reaction zones including the skull and altered regions within the crucible.

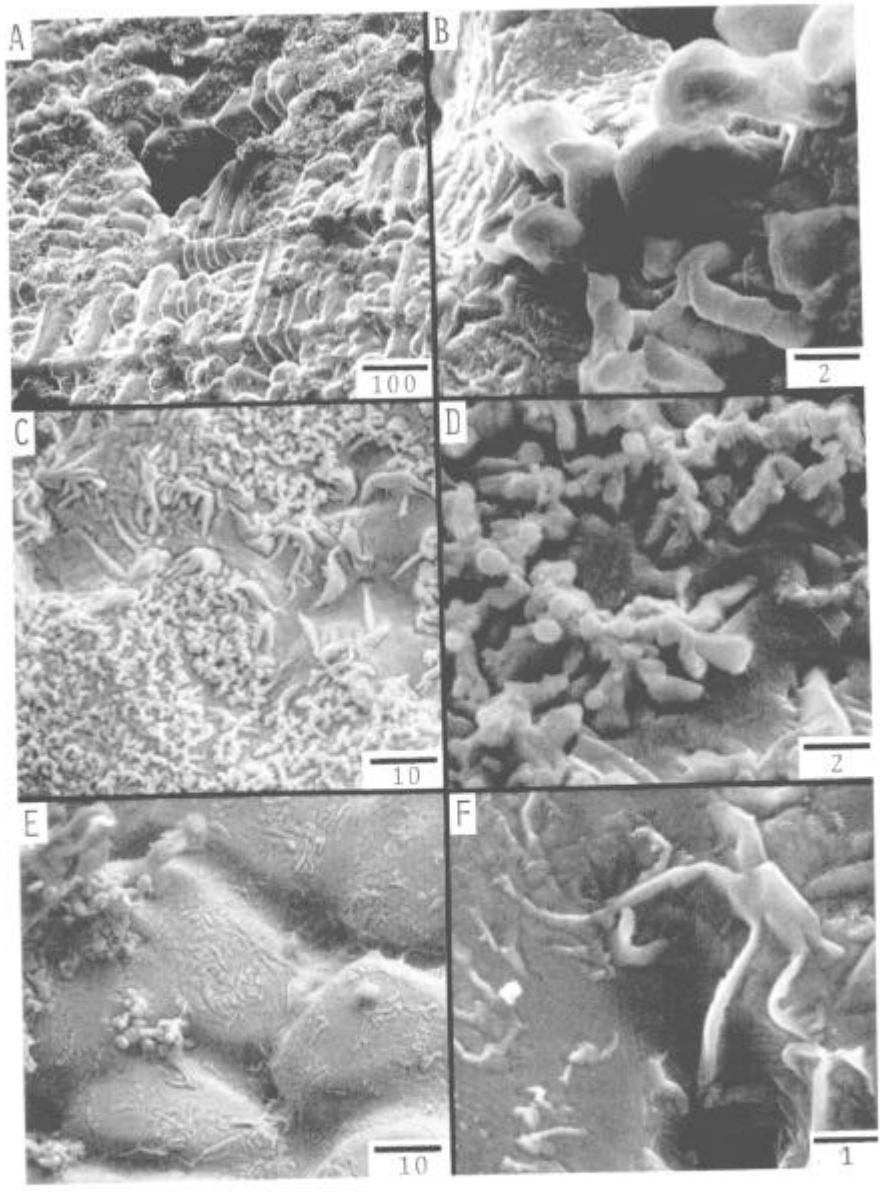

Figure 2. SEM of the melt side of the skull showing exposed oxides on solidified (dendritic) metal surface. Skull from: (A&B) Al_2O_3, (C&D) MgO, and (E&F) spinel crucibles. Note the various types of oxide morphologies. The calibration bar and number indicate the dimensional scale in μm.

Dendrite tips on the MgO-crucible skull are flat compared to the more angular dendrite tips from the Al_2O_3-crucible skull (Fig. 2A). Wormy HfO_2 oxides cover the metal surface in both Figures 2C and 2D. The oxides are almost exclusively HfO_2 and are imbedded in the metal surface. On the flat metal dendrite tips, the HfO_2 has a wormy appearance, while the interdendritic regions, shown in Figure 2C, contain larger HfO_2 particles.

Figure 2E shows the metal side of the skull from the spinel crucible. Flat metal dendrite tips are quite apparent. Several oxides are present on the metal surface. The HfO_2 has two morphologies: wormy oxides deeply rooted in the metal dendrites and spherical particles. Figure 2F shows the wormy oxides in greater detail. The lighter wormy oxides appear to be HfO_2, while the darker ones appear to be predominantly Al_2O_3. These oxides coexist in thin layers with the Al_2O_3 being closer to the metal skull surface, and the HfO_2 existing on top of the Al_2O_3, towards the melt interior. All skulls contain varying amounts of the spherical or chunky HfO_2 particles; however, the wormy HfO_2 particles occur predominantly on the spinel-crucible skull surface.

Figure 3 shows the refractory side of the skull for all three crucibles. Figure 3A shows the surface of the alumina-crucible skull. A cauliflower structure is quite evident in the central and lower portion of the micrograph, which is actually a two-phase structure as shown in Figure 3B. The ZrO_2 occurs as a thin, plate-like layer attached to a columnar Al_2O_3 phase (Fig. 3B). This ZrO_2 layer forms a discontinuous boundary between the crucible and the skull.

Figures 3C and D reveal the oxide morphology on the refractory side of the MgO-crucible skull, which contain a smooth, semi-continuous ZrO_2 layer that covers the surface. This region of the MgO-crucible skull has the same morphology as the Al_2O_3-crucible skull, with the Al_2O_3 product of reaction residing in a columnar morphology below the ZrO_2 layer.

Figures 3E and F show the refractory side of the spinel-crucible skull. Figure 3E shows the Al_2O_3 columnar structure, which resides between the ZrO_2 layer and the metal in the skull. The ZrO_2 layer comprises the entire surface shown in Figure 3F.

Transverse sections of the skulls are shown in Figure 4. Figures 4A and B are typical of the MgO-crucible skull. Oxides appear to extend across the skull. The large globular oxides are

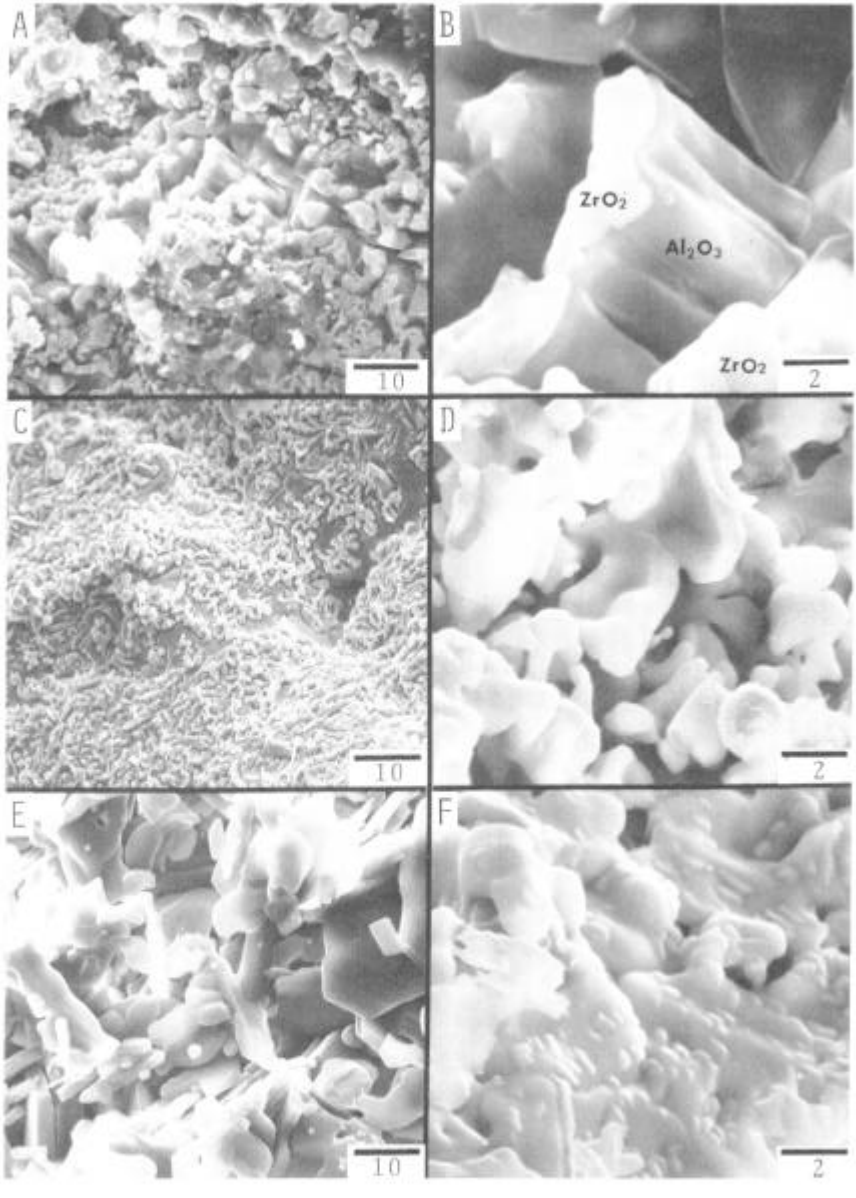

Figure 3. SEM of the crucible side of the skull surface showing heavy concentration of oxides. Skull from: (A&B) Al_2O_3, (C&D) MgO, and (E&F) spinel crucibles. Very little metal is present in this surface.

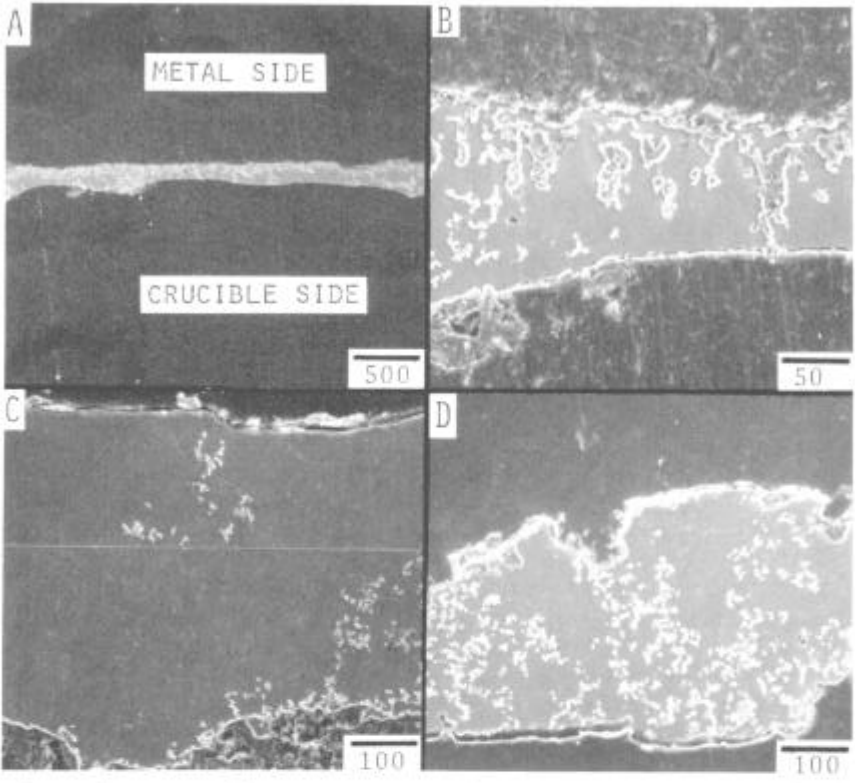

Figure 4. SEM of transverse section of the skulls from (A&B) MgO, (C) Al_2O_3, and (D) Spinel crucibles.

predominantly Al_2O_3, while the smaller spherical oxides are a combination of HfO_2 and Al_2O_3. The view of the skull shown in Figure 4D is dominated by the small spherical Al_2O_3 and HfO_2 particles, which occur throughout the cross section. Figure 4C shows the transverse section of the Al_2O_3-crucible skull; very few fine spherical oxides are present in the metal-side of the skull. The skull from the Al_2O_3-crucible contains few total oxides.

DISCUSSION

When reactive elements, such as Al, Ti, Zr are added to a melt, a complex sequence of reactions occurs, involving the oxidation of these elements at the melt-crucible interface and within the melt. These elements compete with one another for the available oxygen, and the most stable ones (lowest free energy of oxide formation) become oxidized first. In this study, a layer of ZrO_2 was formed first on the grains of

the crucible oxides, as shown in Figure 3B. This is expected, since Zr in a nickel melt will directly reduce pure Al_2O_3 to form a ZrO_2 surface layer (7). Figure 3B indicates that once the ZrO_2 layer reaches a thickness of 1-3μm, an interwoven network of columnar Al_2O_3 forms and grows from the ZrO_2 base into the melt. This sequence is shown schematically in Figure 5, and holds true for the skull build-up in all three crucibles.

The Hf was added late in the melt so that its entry as HfO_2 into the skull occurred only in the outer regions (melt side) as shown in Figure 5. There are several morphologies of the HfO_2 particles, indicating several sources of formation. The HfO_2 particles occur as wormy (Fig. 2C & E), crab-like (Fig. 2F), and rock-like (Fig. 2B & D) structures. Many of the HfO_2 particles are clustered, indicating that they originated as individual particles

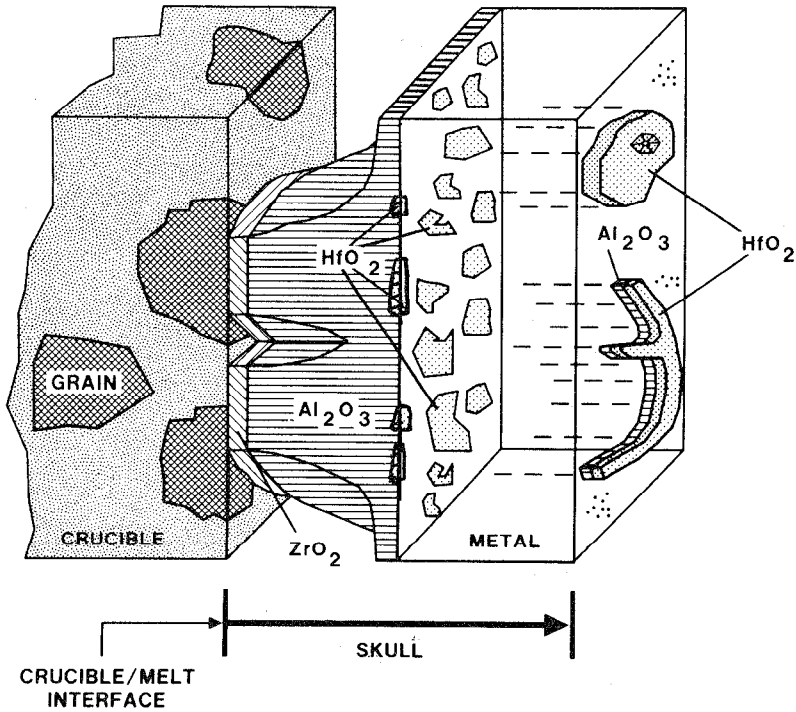

Figure 5. Diagram of progressive oxide build-up in a metal layer to form the skull at the crucible-melt interface.

within the melt, and then coalesced, forming clusters during the stirring of the melt. Eventually they came in contact with the particles in the skull and remained attached as a network of particles. This is indicated in Figure 5 by the numerous HfO_2 particles located on the melt-side of the Al_2O_3 columnar crystals. The clustering phenomenon has been described in a recent publication which shows its effectiveness in removing individual particles from a melt (8). Figure 5 shows some massive HfO_2 particles on the melt-side surface of the skull, where Hf reacted with earlier-formed Al_2O_3 clusters and films. Some of these appear to have originated in the dross, and later became attached to the skull during pouring. Also in Figure 5 are some fine oxide particles rich in Al, Mg, and Cr, which remained attached to the skull surface.

The amount of oxide in the skull varied considerably between the three melts, as shown in Table III. The heat melted in the MgO crucible had the highest level of oxygen (11 ppm) and also had the greatest percent of oxides (50%) in the skull surface facing the melt. The oxides consisted mainly of HfO_2 in the melt-side, and of mixtures of HfO_2 and HfO_2- and ZrO_2-altered Al_2O_3 particles on the crucible side. On the other hand, the skull from the Al_2O_3 crucible was 95% metal with very few HfO_2 crystals (+ clusters) in the melt side surface. Also a scattering of fine Al_2O_3 particles on the melt-side surface were observed (Fig. 2A).

Table III. Data on Skulls and Inclusions

	Skull Surface Melt Side			Skull-Transverse Section			
Crucible	% Metal	% Oxide	Hf/Al Ratio(1)	Avg. Thickness	% Metal	% Oxides	Inclusion Content (Oxides) (5)
Al_2O_3	95	5	0.1	700μm	95	5(2)	1.5ppm
MgO	50	50	8.0	250μm	80	20(3)	6.5ppm
Spinel	90	10	0.5	350μm	80	20(4)	5.9ppm

(1)EDX Peak Ratio;(2) 5% HfO_2+Tr. Al_2O_3;(3) Mixture of HfO_2, HfO_2/Al_2O_3+ZrO_2/Al_2O_3;(4) 10% HfO_2+10% Al_2O_3;(5) Test performed by PWA; Inclusion oxides ∿ to skull oxides, and inclusion content with no reactive adds = 0.35ppm.

CONCLUSIONS

The type and quantity of oxides forming in the melt or at the melt-crucible interface (skull) depend largely on the available oxygen (type of crucible material) and on the amount and types of reactive alloying elements. The

stability (to chemical reduction or dissociation) of the crucible materials decreases in the order: Al_2O_3 > $MgAl_2O_4$ > MgO. Thus, the heat melted in the Al_2O_3 crucible had the least amount of oxides in the skull (predominately HfO_2) and had the lowest inclusion content (1.5ppm, HfO_2). The heat melted in the MgO crucible exhibited the greatest at-pour oxygen, had the greatest amount of oxides in the skull (HfO_2, Al_2O_3, ZrO_2), and had the greatest inclusion content (6.5ppm, HfO_2 + Al_2O_3). The performance of the heat melted in the $MgAl_2O_3$ crucible fell between that of the other two crucibles.

ACKNOWLEDGEMENTS

The authors are grateful to PWA for the work and data on the inclusion measurements, and to W.E. Johnson and G.E. Maurer for their effort in producing the experimental heats.

REFERENCES

1. G.A. Vaughn and G.H. Geiger, "Melt-Crucible Interactions and Inclusion Formation in Vacuum Melted Ni-Al-Ti Alloys," 6th Int. Vac. Met. Conf., San Diego, CA., April 23-27, 1979.
2. W.H. Sutton and D.R. Green, "Influence of Hafnium on the Wetting Characteristics of Mar M-200," Superalloys: Metallurgy and Manufacture, Proc. 3rd Int. Symp.; Claitor's Pub. Div., Baton Rouge, LA, 1976, pp. 171-179.
3. W.H. Sutton and D.R. Green, "Interfacial Reactions Between a Hafnium Containing Nickel-Base Superalloy and Zirconia Ceramics," Ceramic Microstructure '76, Westview Press, Boulder, CO, 1977, pp. 520-531.
4. W.H. Sutton and G.E. Maurer, "Influence of VIM Crucible Composition on Nonmetallic Content of an Advanced Hafnium-Bearing Nickel-Base Superalloy: Part I Crucible Materials, Processing, and Characterization of Reactions," 6th Int. Vac. Met. Conf., San Diego, CA, April 23-27, 1979.
5. E.E. Brown, L.J. Jennings, and R.W. Salkeld, "Part II - Characterization of Inclusions in an Advanced Hafnium-Bearing Nickel-Base Superalloy," ibid.
6. J.E. Stulga and E.E. Brown, "Effects of Vacuum Arc and Electroslag Remelting on the Non-Metallic Inclusion Content of MERL 76, an Advanced Hafnium-Bearing Nickel-Base Superalloy," This Symposium, Seven Springs, PA, Sept. 21-25, 1980.
7. W.H. Sutton and E. Feingold, "Role of Interfacially Active Metals in the Apparent Adherence of Nickel to Sapphire," Materials Science Research, Vol. 3, Plenum Press, 1966, pp. 577-611.
8. T.B. Braun, J.F. Elliott, and M.C. Flemings, "The Clustering of Alumina Inclusions," Met. Trans. Vol. 10B, June, 1979, pp. 171-184.